La mer 58 : 17–33, 2020, https://doi.org/10.32211/lamer.58.1-2_17
Société franco-japonaise d'océanographie, Tokyo

Effect of wind on seawater exchange in Matsushima Bay

Huang JIANXI[1], Kohei MIZOBATA[2] and Yujiro KITADE[2] *

Abstract: To examine seawater exchange in Matsushima Bay, we analyzed monthly temperature and salinity data, obtained by the Miyagi Prefecture, and temperature monitoring data provided by the Sena and Varns Corporation. The difference in surface temperature, between water inside and outside of the bay, is larger in early summer and late summer, and decreases in mid summer, indicating two peaks in the warming season. A temperature fluctuation with a several-day period was strongly correlated to the northwest-southeast wind component, which dominated from early summer to fall. The correlation indicates that the temperature decrease was induced about 2 days after southeastward wind events. In order to clarify these mechanisms, we employed the Regional Ocean Modeling system (ROMS) using observed atmospheric data. After reproducing the temperature variation from spring to fall, we found that over a several-day period, wind induced seawater exchange and variation in the temperature difference between water inside and outside of Matsushima Bay. Monitoring data and model results confirmed that an internal tide was generated in the bay during the formation of a thermocline that occurred after the southeastward wind. These results indicate that wind-induced seawater exchange occurs in Matsushima Bay.

Keywords : *seawater exchange, wind effect, internal wave, ROMS*

1. Introduction

Matsushima Bay is located in the northwest of Sendai Bay, Japan, which is connected to the Pacific Ocean (Fig. 1). The width of the mouth of Matsushima Bay (w) is about 1.7 km, and the area (s) is approximately 35.3 km^2. The maximum depth in the bay mouth (d_1) and the water depth inside Matsushima Bay (d_2) are both approximately 4 m (average depth = about 3 m). According to the formula for the geographical enclosed index ($r = d_2\sqrt{s} / d_1 w$; WADA, 1989), the index for Matsushima Bay is approximately 3.5. From the table of geographical enclosed indices (INTERNATIONAL EMECS CENTER, 2001), the indices for Tokyo Bay and Osaka Bay are 4.2 and 3.4, respectively. Since a geographical enclosed index greater than 2 indicates that a bay is enclosed (WADA, 1989), Matsushima Bay is categorized as an enclosed bay, like Osaka Bay.

Matsushima Bay is a famous oyster-cultivation area, but high oyster mortality has been reported in recent times. An exceptionally low oyster seedling yield was recorded in 2013, despite a higher density of early-stage larvae than

---

1) IDEA Consultants, Inc.
2) Department of Ocean Sciences, Tokyo University of Marine Science and Technology
＊Corresponding author:
E-mail: ykitade@kaiyodai.ac.jp

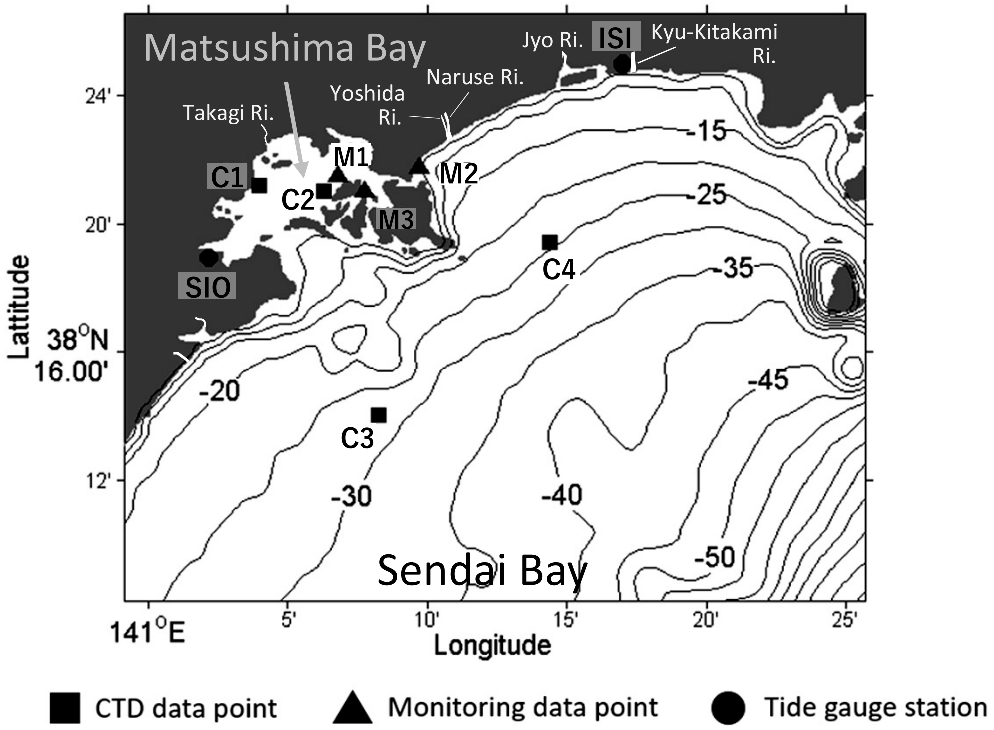

Fig. 1 Locations of monthly CTD observation stations (C1 to C4), monitoring stations (M1 to M3), and tide-gauge stations (SIO and ISI) in the northwest of Sendai Bay.

in previous years. Kakehi et al. (2017) reported that the unusually low surface salinity in August 2013 enhanced estuary circulation, and early-stage oyster larvae were transported out of the bay before they reached the pre-attachment stage. Thus, the oyster seedling yield is thought to be closely related to seawater exchange in northwestern Sendai Bay. To understand the advection and diffusion of seedlings, it is necessary to clarify the mechanism of seawater exchange.

Previous studies have indicated that estuary circulation and tidal current are important processes for seawater exchange in Matsushima Bay. Shirai et al. (2019) conducted a high-resolution numerical experiment on Matsushima Bay and clarified the process of low-salinity water flowing into the surface waters of the bay. The effect of wind, as an external force, was included in the numerical simulation conducted by Shirai et al. (2019), but the effect of wind on circulation and water exchange was not explicitly discussed. Although numerical experiments have been conducted, the mechanisms of seawater exchange between Matsushima Bay and Sendai Bay remain an unsolved issue. Wind-driven circulation sometimes dominates in enclosed bays, such as in Tokyo Bay in the weak river-discharge season (Nagashima and Okazaki, 1979; Guo and Yanagi, 1995; 1996). Wind forcing can act as a direct driving force of current and circulation in Matsushima Bay, while the rotation effect is not essential to circulation in such a small bay. In this study, we examine the characteristics of water condition and wind variation related to water exchange, and then attempt to explain them using a numerical model.

2. Observational data

To examine oceanic conditions within Matsushima Bay and Sendai Bay, we analyzed a dataset of temperature, salinity, and dissolved oxygen (DO) measurements, recorded in this area from 2014 to 2017, along with sea level data and meteorological data (Fig. 1). The Matsushima Bay data were obtained by Conductivity Temperature and Depth profiler (CTD) by the Miyagi Prefectural Government once every two months, while the Sendai Bay data were obtained once a month. Sea level data were collected at the Shiogama (SIO, Fig. 1) and Ishinomaki (ISI, Fig. 1) stations by the Japan Meteorological Agency (JMA). Precipitation data were collected at the Shiogama and Ishinomaki stations through the Automated Meteorological Data Acquisition System (AMEDAS) maintained by the JMA. In this area, a monitoring buoy system constructed by the Sena and Vans Corporation observed sea surface temperature (SST) once every hour from April 2nd, 2016 to March 30th, 2017 at three locations (Fig. 1). This SST dataset was used to examine inter-seasonal variation with high temporal resolution.

3. Characteristics of observational data

3.1 Temporal variability of seawater properties

The time series of temperature, salinity, and DO recorded at C1 at the surface and bottom of Matsushima Bay (Fig. 2a), clearly show seasonal temperature variability, with the lowest temperatures recorded in February and the highest recorded in August. The temporal variability of salinity and DO are similar but show opposite variation to that of temperature, i. e. low in summer and high in winter. All water properties indicate a homogeneous water structure at C1. Figure 2b shows the time series of the same properties observed at C3 at depths of 0 m (surface), 10 m, and 20 m. The difference in temperature between 0 m and 10 m, or 20 m, shows that temperature stratification was strongly developed between April and September, but became disrupted from October. The highest temperature occurred in August every year. Salinity at the sea surface was lower than at other depths, and a decrease in salinity occurred in July. However, abnormally low salinities were recorded at the surface in 2016 and 2017. The AMEDAS data indicate this was related to rainfall that occurred before the observation date (not shown). At a depth of 20 m, the lowest DO occurred in September, while the lowest DO at 0 m and 10 m was recorded in August. The measurements indicate that there is little difference between the surface and bottom layers in terms of DO. Although Matsushima Bay is geographically classified as a closed bay, the almost-uniform vertical distribution of DO during the summer stratification period suggests there was enhanced vertical mixing.

There is a slight difference in temperature between the waters of Matsushima Bay (Fig. 2c, upper panel) and those obtained from the rest of Sendai Bay. The temperature difference between C3 and C1 was therefore investigated (Fig. 2c, lower panel). The temperature difference showed two peaks during the warming period (from April to August). This is an interesting feature because during the warming period, the temperature within the bay is expected to be generally higher than that outside the bay. If both areas receive the same amount of heat, the inner bay, with a smaller heat capacity, will heat up more than the open sea. The heat capacity of Matsushima Bay, which is semi-enclosed and shallow, is smaller than that of Sendai Bay, but shows two peaks every year, implying that something induced relative heat loss in Matsushima Bay, or relative heat gain in Sendai Bay.

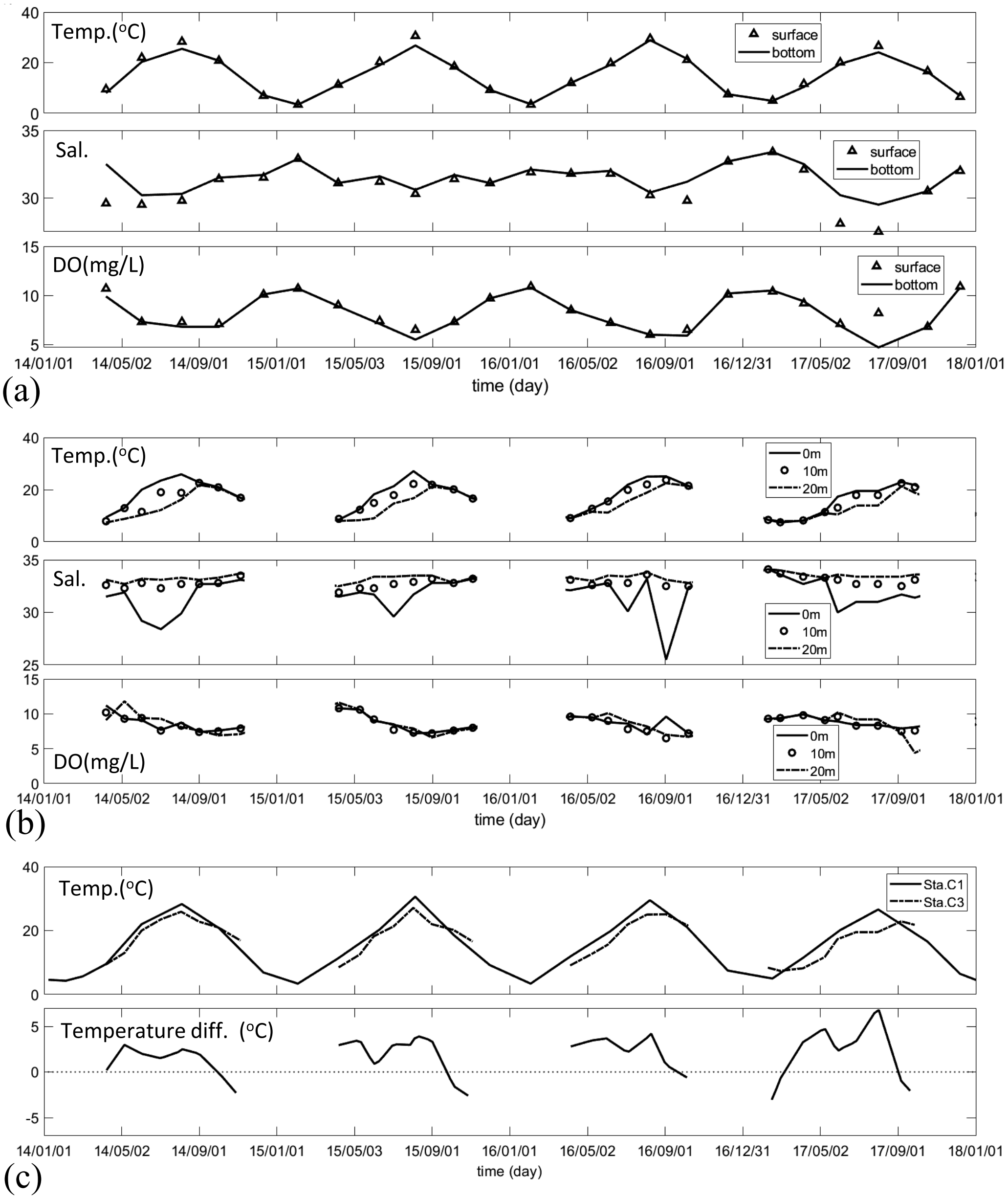

Fig. 2 Time series of temperature, salinity, and dissolved oxygen observed by the Miyagi Prefectural Government at (a) C1 and (b) C3 in Matsushima Bay. (c) Time series of surface temperature at C1 and C3, and temperature difference between C1 and C3. Two peaks in temperature difference are notable in the warming season every year.

Based on the spatial scale of the study area, the two peaks of temperature difference (Fig. 2c, lower panel) are difficult to attribute to heat flux from the atmosphere. Hence, it may be related to the differences in seawater exchange between these two areas. Thus, we tried to approach the

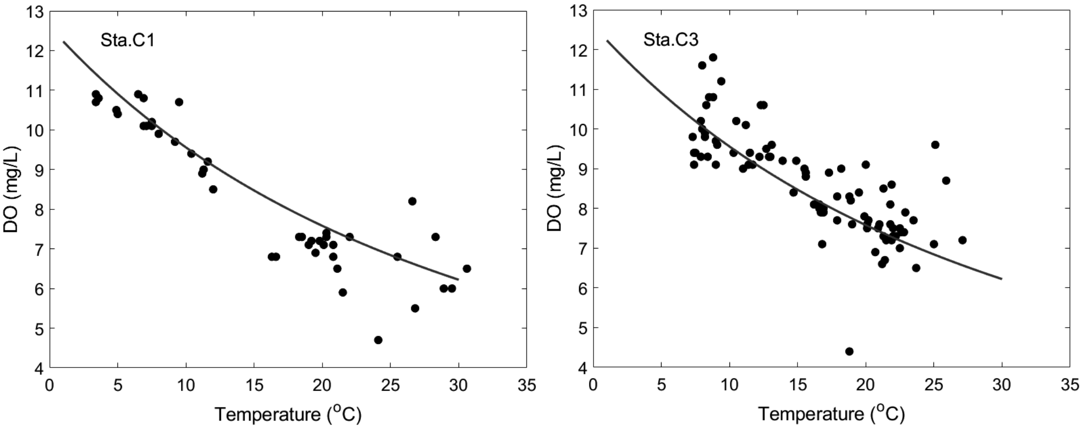

Fig. 3 Relationship between seawater temperature and DO, at inside（Sta. C1）and outside（Sta. C3）of Matsushima Bay. The black curve is the dissolved oxygen saturation curve.

mechanism of seawater exchange by understanding this twin-peak mechanism.

Because DO fluctuates seasonally and is low in summer, it is important to confirm whether low-DO water is also formed in the bottom layer of Matsushima Bay. This would indicate the strengthening of summer stratification, which is often observed in other enclosed sea areas such as Tokyo Bay. Figure 3 shows the relationship between temperature and DO at C1 and C3. The black curve is the dissolved oxygen saturation curve, which is calculated using the dissolved-oxygen formula（Weiss, 1970）. The observation data were distributed around the curve, indicating that DO was saturated during the study period. That is, although DO is low in summer, the water mass of Matsushima Bay is not extremely deoxygenated, even during summer stratification, suggesting that there is moderate mixing between inner bay seawater and river water or seawater outside the bay.

We compared the daily mean water temperatures from March 2016 to November 2016, obtained at M1 and M2 using a monitoring system, with those recorded at C2 and C4（CTD data）（Fig. 4）. The water temperatures at M1 and M2 are generally similar to those at C2 and C4. Features of the CTD data are also evident, such as the rise in temperature towards August, and higher temperatures inside the bay than outside the bay. Although monitoring was conducted near the shore, the water temperature observed by the monitoring system suggested to be representative of the broader sea area. The continuous water temperature monitoring data shows remarkable several-day fluctuations in addition to seasonal fluctuations.

3.2 Wind data characteristics

The relationship between several-day temperature fluctuations and the local wind conditions was examined because the several-day fluctuations（Fig. 4）were thought to be related to the wind along the east coast of Honshu（Kitade et al., 1998; Kitade and Matsuyama, 2000）. Figure 5a shows that the predominant wind direction was from the northwest, between October and December. From April to September, the winds in the northwest of Sendai Bay showed more variation, with the wind rose diagram（Fig. 5b）indicating that the wind was mainly from the northwest and the southeast, approximately 23%

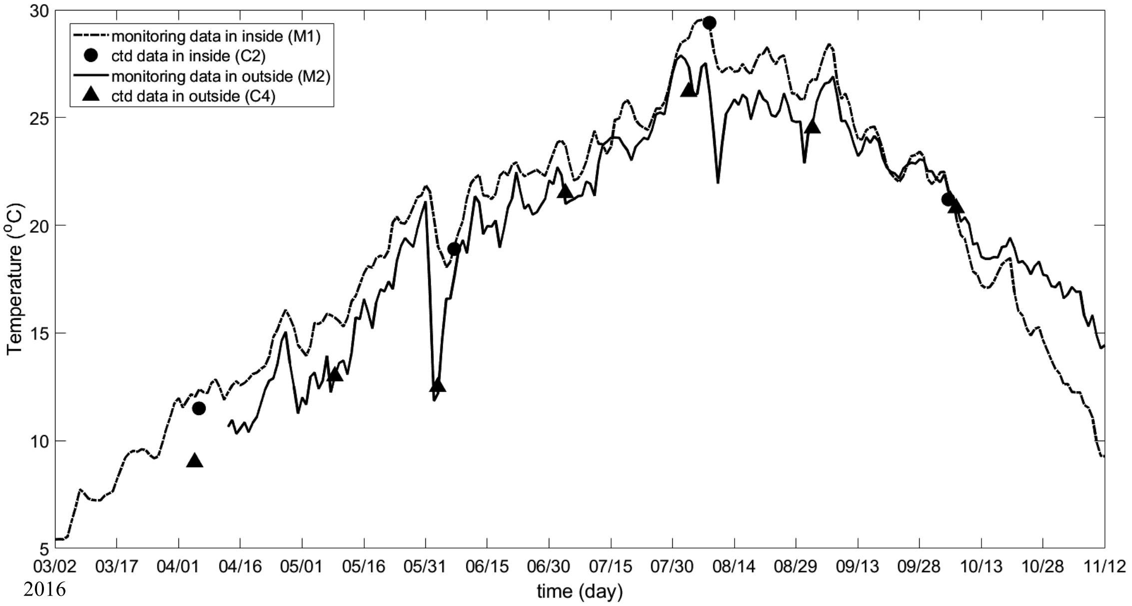

Fig. 4 Time series of daily average temperature obtained by the monitoring system at M1 and M2. The surface temperature observed by the Miyagi Prefecture Government is also indicated by the symbols ● and ▲.

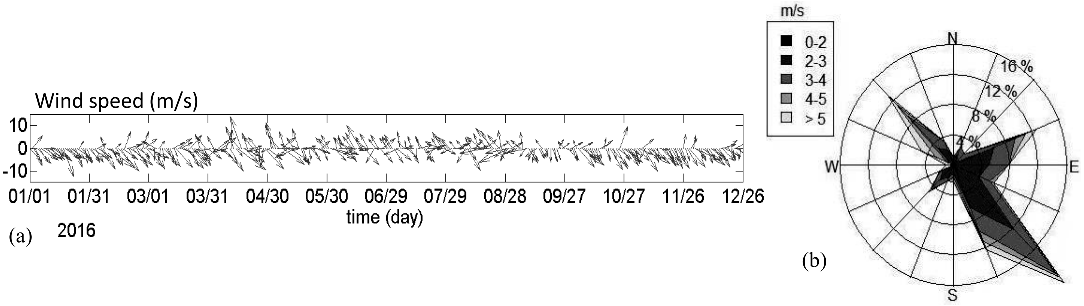

Fig. 5 (a) Time series of wind vectors. (b) Wind rose diagram from April to September 2016.

and 13%, respectively. The cross-correlation between the northwest-southeast component of the wind and the water temperature fluctuations was examined using a band-pass filter data from 25 hours to 10 days (Fig. 6). In all months except June, the absolute value of the correlation coefficient is highest in the negative time lag region, when the water temperature fluctuation occurs after there has been significant wind blowing. The negative correlation coefficient implies that an SST minimum was typically induced between 24 h and 75 h after the northwest wind maximum (Table 1). The correlation coefficient and time lag fluctuate from month to month, but this is expected, as the water temperature distribution and stratification, within the bay and beyond it, are not always the same. These results suggest that the seawater exchange and stratification in Matsushima Bay is related to the northwest-southeast component of the wind.

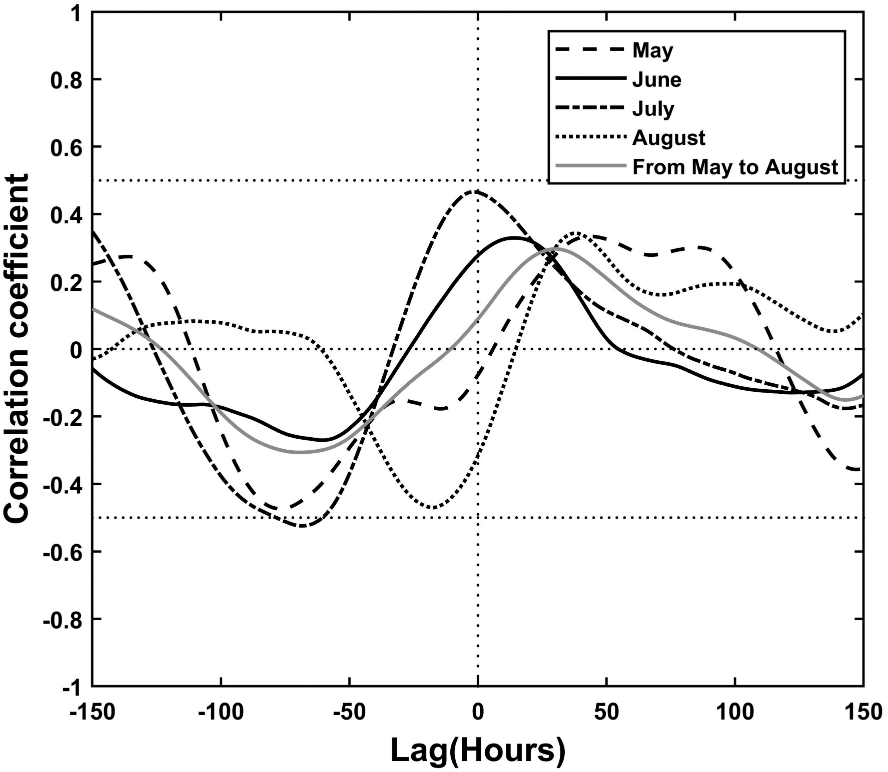

Fig. 6 Lag correlation between northwest-southeast component of wind and temperature fluctuation. A band-pass filter of 25 h - 10 days was applied to both wind and temperature data. A negative time lag indicates that the temperature fluctuation occurs after the wind has been blowing.

Table 1. Lag correlation between northwest-southeast wind component and temperature fluctuations over several-day periods.

	May	Jun	July	August	May-Aug.
Correlation coeff.	−0.45	−0.3	−0.5	−0.45	−0.4
Time Lag (hour)	75	50	60	24	60

3.3 Summary and discussion of the observational results

In the northwest of Sendai Bay, the temperature stratification gradually increased during the warming season, as shown in Fig. 2. Since the specific heat capacity of Matsushima Bay is much less than that of the rest of Sendai Bay, Matsushima Bay experienced a more significant temperature increase during the warming season. A decrease in DO during the warming season was related to a decrease in saturated oxygen due to the increase in temperature. According to CTD data, the difference in sea surface temperatures, between water inside and outside of Matsushima Bay, shows two peaks in the warming season. Continuous monitoring data indicated that the water temperature fluctuated over a period of several days, and that the fluctuation was well correlated with the northwest-southeast wind component. This suggests that the wind causes inflow and outflow of seawater through the Matsushima Bay mouth, resulting in seawater exchange and limiting stratification of the bay.

However, some unexplained aspects of this phenomenon remain, including: 1) how the unsteady winds, that blow from different directions between April and September, affect seawater transport and temperature; 2) the mechanism responsible for the two peaks in the temperature difference between water inside and outside of Matsushima Bay; 3) the relationship between tide and seawater exchange in the northwest of Sendai Bay. Because the observation data are insufficient to clarify these unknowns, we will use a numerical model to answer these questions.

4. Modeling and reconstruction

4.1 Model and conditions

The Regional Ocean Modeling system (ROMS) used in our experiment is a three-dimensional nonlinear primitive equation model, which is a modified and improved version of the SCRUM (the *S*-coordinate Rutgers University Model) developed by Rutgers University and University of California, Los Angeles. The model state variables were staggered using an Arakawa C-grid. ROMS uses an *s*-coordination system for vertical discretization, which considers the surface change in the σ-coordination system. The ROMS governing equations are discretized over variable topography using a stretched, terrain-following, vertical coordinate.

The model area covers the northwest region of Sendai Bay (latitude: 38.0423° N - 38.5089° N, longitude: 140.9263° E - 141.5346° E, Fig. 7a). The coastline is drawn from the data of the Global Self-consistent, Hierarchical, High-resolution Shoreline Database (GSHHS). The bathymetry dataset used in this study is JTOPO30, distributed by the Marine Information Research Center of the Japan Hydrographic Association (http://www.mirc.jha.jp/products/JTOPO30v2/). The dataset has a horizontal resolution of 0.0041° × 0.0041° (black grid in Fig. 7b), and the vertical direction was divided into ten layers. The model represents the period from January 1st to De-

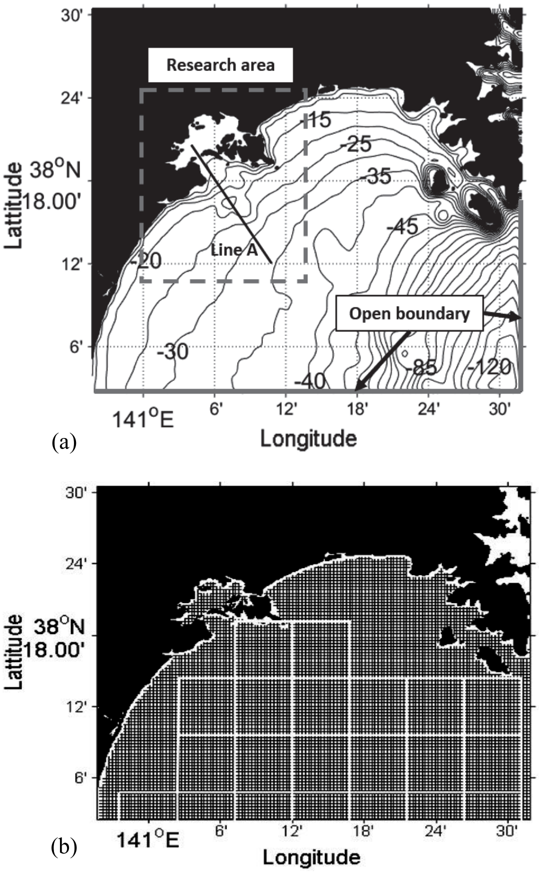

Fig. 7 (a) The model area and main research area (dashed gray line), and the south and north boundaries (solid gray line) that were set as open boundaries. (b) Distribution of the horizontal grid. The black and white grids are from ROMS and HYCOM, respectively.

Table 2. Boundary conditions applied in the model.

	Open boundary	Coastal boundary
Surface elevation	Chapman B.C.	Close
2-D velocity	Flather B.C.	Close
3-D velocity	Clamped B.C.	Close
Energy scattered	Gradient B.C.	Close

cember 31st, 2016 as continuous monitoring data is limited to 2016. The initial conditions and boundary conditions for temperature and salinity were provided by the World Ocean Atlas 2009 (WOA2009, global grid 1° × 1°, monthly) and by HYCOM + NCODA Global Reanalysis (resolution: 1/12°, latitude: 37.04°N - 39.04°N, longitude: 140°E - 142.96°E), respectively. The high-resolution ROMS required approximately 7 days of spin-up time at the boundary areas. The boundary conditions for two-dimensional or three-dimensional velocity, surface elevation and scattered energy were as per the conditions of FLATHER (1976) and CHAPMAN (1985), and are presented in Table 2.

The sea surface heat and freshwater flux conditions were determined from daily reanalysis data of the National Centers for Environmental Prediction (NCEP-DOE AMIP-II reanalysis-2, global grids at varying resolutions), and daily precipitation data obtained by the JMA. These datasets were temporally interpolated and applied homogeneously in our model area at every time step. The daily wind data obtained by the JMA were also temporally interpolated and were applied homogeneously as sea surface wind stress conditions.

Eight constituent tides (M2, S2, N2, K2, K1, O1, P1, and Q1) were added on the open boundary from the TPXO7 dataset (http://volkov.oce.orst.edu/tides/TPXO7.2.html) to drive the seawater movement. The correlation coefficients (R) between observations and model results, for sea level fluctuation at Ishinomaki and Shiogama, were 0.95 and 0.96, respectively. Variation in surface tide was well reproduced by this model.

Simulated results and comparison with observational data

In this subsection, we examine the reproducibility of the model by comparing water temperature and salinity fluctuations, and fluctuations in SST differences within Matsushima bay and beyond it.

First, the seasonal variations in water temperature and salinity at the CTD stations were compared with the model results (Fig. 8). While water temperature and salinity are almost vertically uniform in Matsushima Bay due to its shallow depth (Fig. 8a), stratification formed outside the bay from April (Fig. 8b). The model exhibits similar vertical differences in both temperature and salinity to those observed by the CTD stations (Fig. 8b). Therefore, the seasonal changes in water temperature and salinity observed by CTD have been reasonably reproduced by the model.

The model-calculated temperature difference, between Matsushima Bay and the rest of Sendai Bay, was compared with the temperature differences from the CTD data, as was the northwestern wind component. The fluctuation in temperature difference (Fig. 9a) seems to correspond to the three-day moving averaged wind (Fig. 8b, black line). When the wind is from the southeast (negative value of wind), the temperature differ-

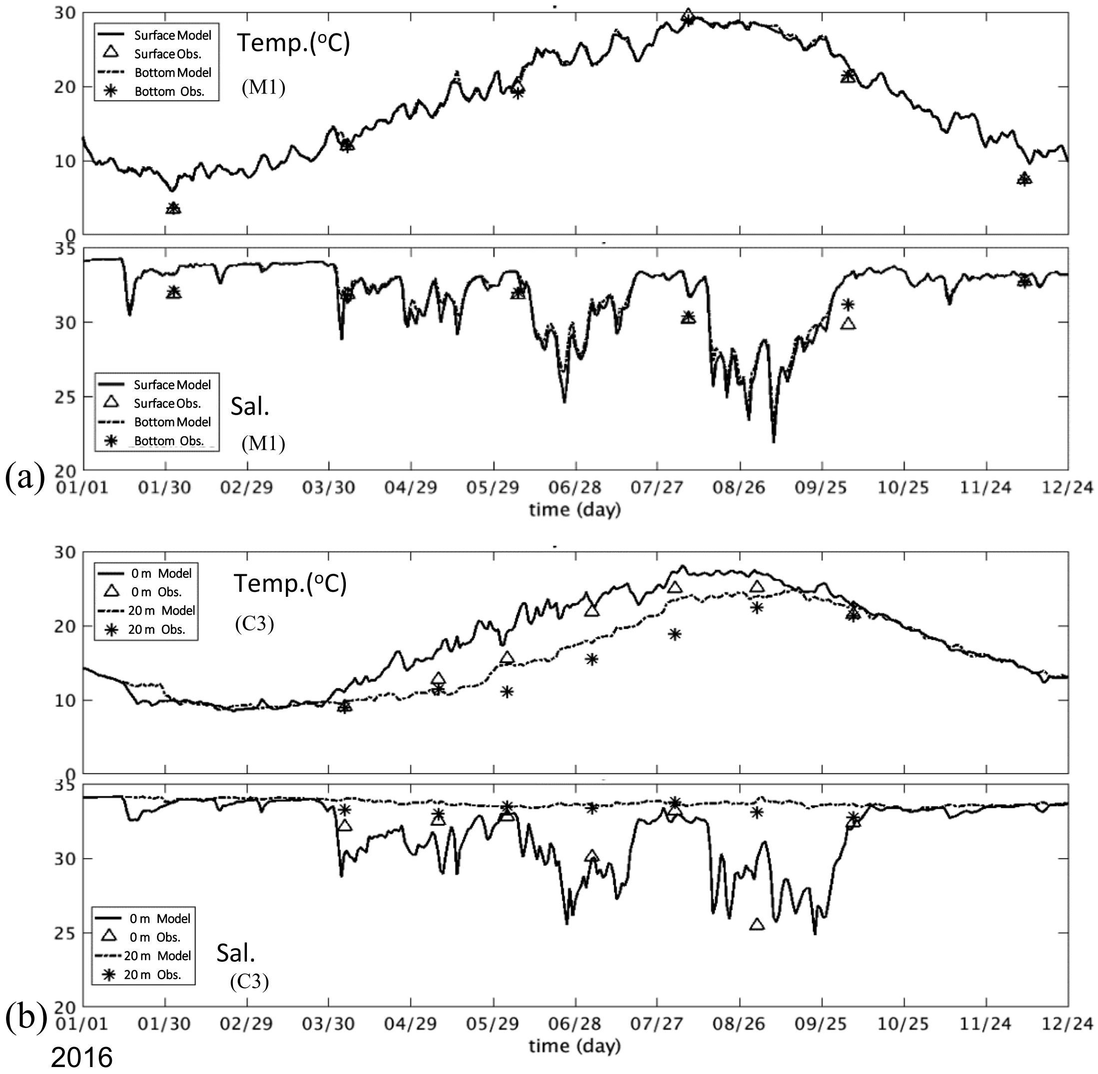

Fig. 8 Comparison between model results and observations from (a) Matsushima Bay and (b) the rest of Sendai Bay. Surface values calculated by the model are indicated by solid and dotted lines. The surface values obtained by the CTD observation are indicated by a triangle and an asterisk.

ence tends to increase. On the contrary, when the wind is from the northwest (positive value), the temperature difference tends to decrease. Although the absolute value of the water temperature is higher in the observed CTD data than in the model, the seasonal variation characteristics are reproduced without contradiction. For example, the temperature difference is larger in periods I and III than in period II, in both the CTD data and the model. Periods I and III correspond to wind from the southeast, while period II corresponds to wind from the northwest. In other words, the temperature difference is large when the wind blows from the southeast, towards the bay, and small when the wind blows from the northwest, away from the bay.

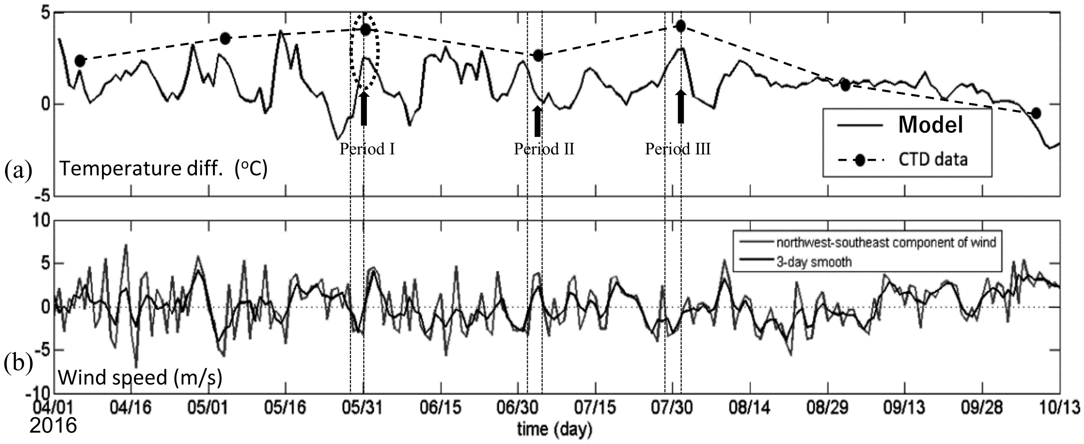

Fig. 9 (a) The time series of the difference in surface temperature between C1 and C3. The black points and solid lines are the CTD data and the model results, respectively. (b) Time series of the northwest-southeast wind component, where the gray line is the daily data, and the black line is the 3-day smoothed data. A positive wind value indicates wind blowing from the northwest.

5. Discussion

5.1 Two peaks observed in the warming season

Using Period I (May 27th to May 30th) as an example, we show how coastal water responds to the wind, in terms of horizontal and vertical distribution of water temperature and current velocity (Fig. 10). Figure 10 shows the distribution of model-derived seawater temperatures after the application of a 25-hour moving average filter, to remove the effects of the tidal cycle. According to the model, on May 27th, the wind was weak but blowing southeastward and stratification had formed in the bay. On May 28th, the wind direction became northwestward, indicating that inflow occurred within the surface layer through the narrow bay mouth. On May 29th, the northwestward wind became stronger, and the stratification in the bay almost disappeared.

The distributions of temperature and velocity for Periods I, II, and III are shown in Fig. 11. The top of Fig. 11 shows the distribution of the following day (May 30th). The inflow into the bay was weak, and the cross section shows that the water temperature stratification disappeared within the bay. The temperature inside the bay was almost uniform, at 20 °C or higher, but the thermocline was inclined, so the temperature difference between water inside and outside of the bay increased significantly. When the wind was towards the southeast, the bay water flowed out, and the coastal water responded in an almost-opposite direction, strengthening the stratification in Matsushima Bay and equalizing the SSTs of water inside and outside of the bay (Fig. 11, period II). In periods I and III, when the wind was towards the northwest, the temperature was almost vertically uniform in the bay and the SST difference between the inside and outside was large. On the other hand, in period II (southeastward wind), stratification occurred in the bay and the SST difference was small.

This demonstrates that the wind affected the variation in temperature difference between water inside and outside of the bay during the warming season. While fluctuations in winds

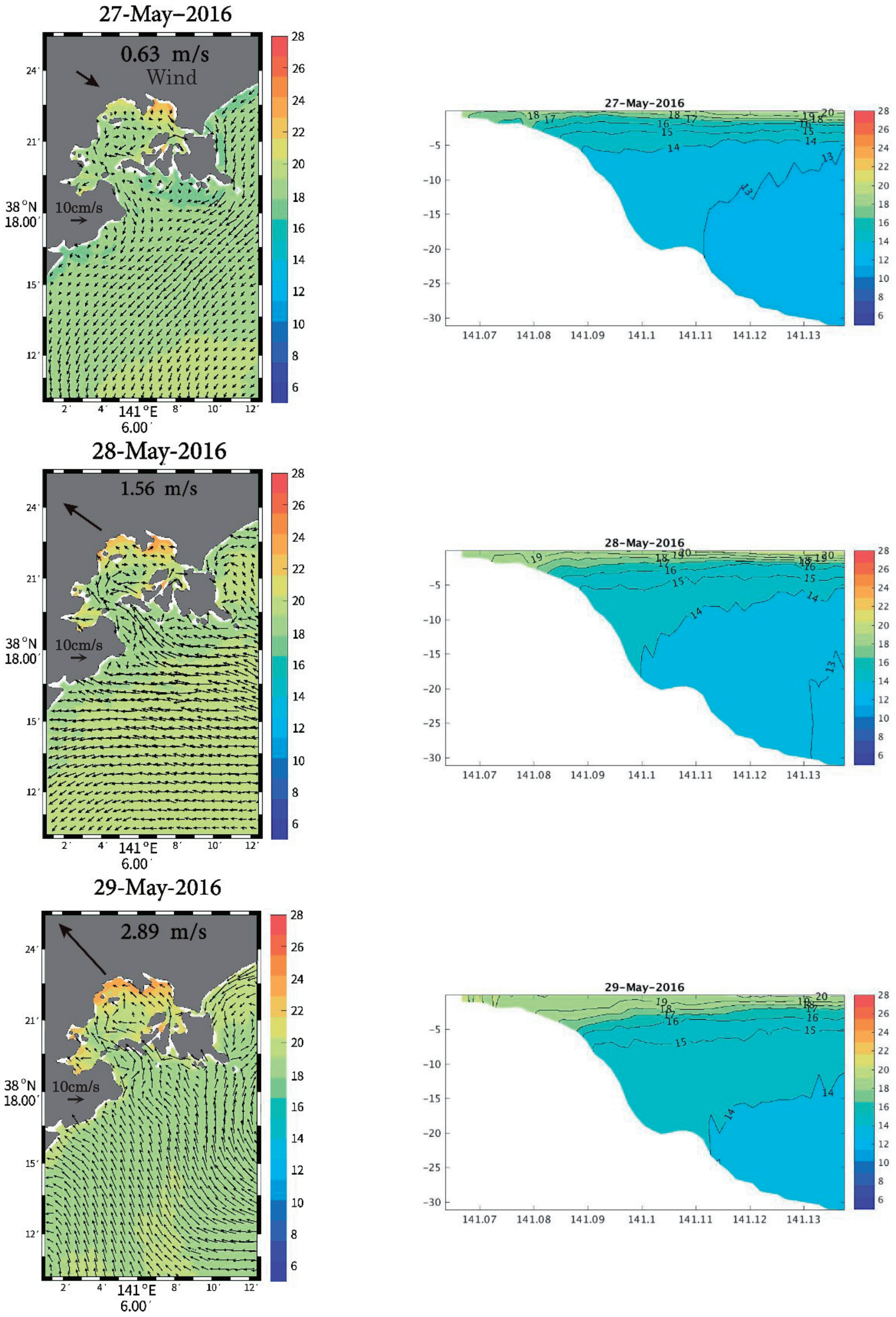

Fig. 10 Plan views (left) and vertical sections (right; taken along Line A in Fig. 7) of seawater temperature distribution between May 27th to 29th, 2016. All figures were drawn after applying a filter to the data, to remove tide effects.

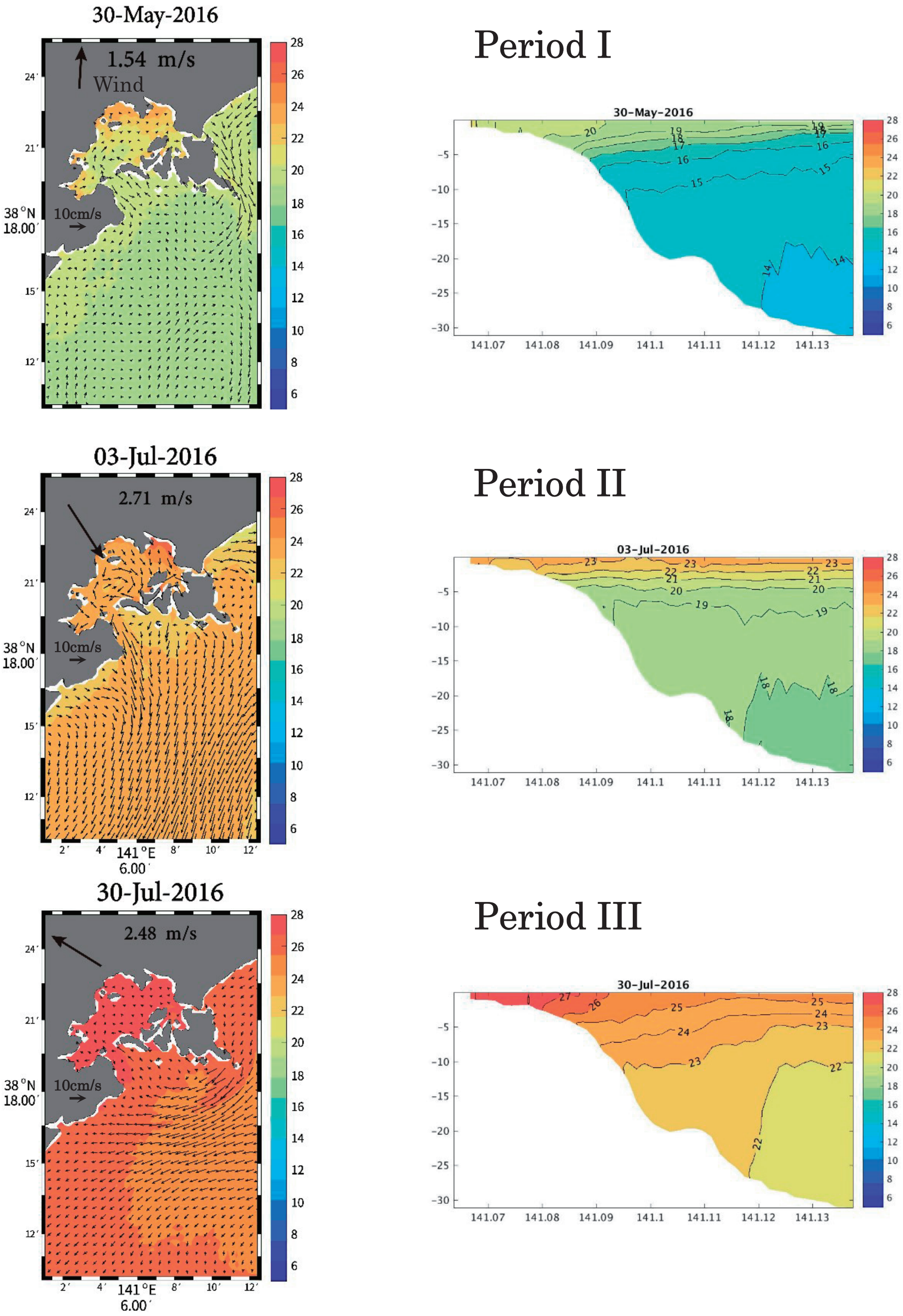

Fig. 11 Plan views (left) and vertical sections (right; taken along Line A in Fig. 7) of seawater temperature distribution for Period I, II and III. All figures were drawn after applying a filter to the data, to remove tide effects.

with several-day period cause periodical SST differences, the CTD data only obtained once in a month. The appearance of two peaks during the warming season itself is probably a type of aliasing feature. In other words, it is not important that there were two peaks, but the research conducted to investigate their characteristics revealed that wind contributes to seawater exchange in Matsushima Bay.

5.2 Relationship between tidal variation and seawater temperature

From the previous section, it is clear that stratification occurred in the bay in response to the southeastward wind. Although only the sea surface temperature was obtained by the monitoring system, it is speculated that if an internal tide variation is formed in Matsushima Bay due to the strengthening of stratification, its signal might also be captured in the SST variation. Therefore, we applied a band-pass filter, for the semidiurnal period band, to SST data obtained by the monitoring system and examined the resulting water temperature fluctuation (Fig. 12). Here, only the semidiurnal period band is extracted, so as to prevent the influence of the internal Kelvin wave of the diurnal period and/or the inertial period, which is propagating outside the region of Matsushima Bay, from being included in the data.

Semidiurnal period fluctuations were intermittently amplified at monitoring stations M1 and M3 (Fig. 12c). Here, the black lines, which indicate the amplitude of temperature fluctuation, were clearly related to wind variation (Fig. 12d). The amplification of semidiurnal temperature fluctuation appears approximately 2 days after the southeastward wind. It is reasonable to consider the amplification of the semidiurnal period fluctuation in temperature as being induced by the generation and propagation of internal tides in stratified Matsushima Bay. The model results also show amplification of the semidiurnal internal tide occurring 2 days after the southeastward wind (Fig. 12b). These results support the idea of wind-driven seawater exchange in Matsushima Bay.

5.3 Seawater exchange in Matsushima Bay

The model revealed that wind caused a change in the stratification of the bay, and the observational results also confirmed the signals of the semidiurnal internal waves. Therefore, using the model results, we calculated the seawater exchange rate caused by wind in Matsushima Bay. Table 3 shows the inflow into Matsushima Bay for Periods I, II, and III using the 25-hour running average velocity data from the bay mouth. It was found that there was an inflow of $3.5 \times 10^6 \sim 9.89 \times 10^6$ m^3/day. This flow volume becomes a flow velocity of 1.2–3.4. cm/s when the width and half-depth of the bay mouth are about 1.7 km and 2 m, respectively. While the current velocity at the bay mouth is quite small, the seawater exchange rate of Matsushima Bay over 3 days would be about 15%, and we could not ignore the effect of wind-driven seawater exchange. Namely, the wind-induced water exchange might be as much as 5% of the total volume of Matsushima Bay per day. Effect of river water was suggested to affect the water exchange in Matsushima Bay (Kakehi et al., 2017; Shirai et al., 2019). Because river water discharge was not included in this model experiment, only the effects of wind-induced seawater exchange are evaluated here. However, the effect reentering of outflow water must be considered in the case of wind-driven water exchange because a set of inflow and outflow was induced by the wind with several-day period. Since the outflow water from Matsushima Bay would be affected by the flow outside

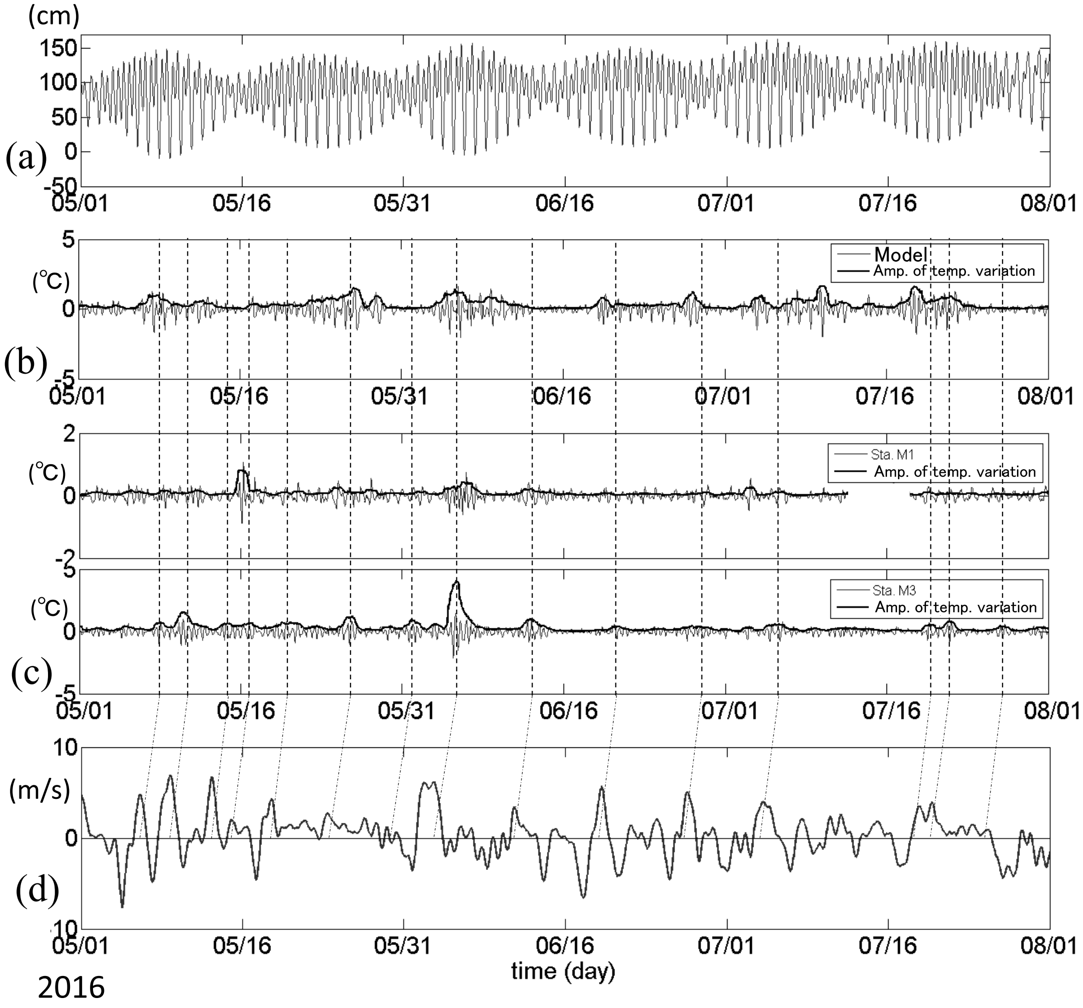

Fig. 12 (a) Time series of sea level at SIO. (b) Time series of semidiurnal band-pass-filtered temperature at M3 calculated from the model data. (c) Time series of semidiurnal band-pass-filtered SST at M1 and M3. (d) Time series of the northwest-southeast wind component. A positive wind value indicates wind blowing from the northwest.

Table 3. Inward water transport and seawater exchange rate for each period after a wind event.

Period	I		II		III	
Daily inward transport	May 28	4.36×10^6	July 1	5.59×10^6	July 28	3.76×10^6
[m^3/day]	29	4.48×10^6	2	3.50×10^6	29	4.74×10^6
	30	5.66×10^6	3	9.89×10^6	30	7.10×10^6
3-day total [m^3/day]		14.50×10^6		19.00×10^6		15.61×10^6
3-day exchange rate*		13.4 %		17.6 %		14.5 %

*3-day exchange rate = 3-day Total in follow vol.／ Volume of Matsushima Bay, where volume of Matsushima Bay is about $1.08 \times 10^8 m^3$.

the Bay, it is speculated that there is little re-inflow of water into Matsushima Bay. The discussion on the re-inflow rate is left to future studies. We would like to point out in this article that per wind event, about 15% of the seawater in Matsushima Bay might be exchanged as a result of wind. More detailed investigations in the future will require appropriate arrangements of monitoring systems, and the use of reproduction models.

6. Summary and conclusion

To examine the properties of seawater exchange on Matsushima Bay, we investigated monthly temperature and salinity datasets obtained by the Miyagi Prefecture, and temperature monitoring data provided by the Sena and Varns Corporation. The difference in surface temperature, between water inside and outside of the bay, is large in early summer and late summer and decreases in mid summer. Thus, it displays two peaks in the warming season. The temperature fluctuation over a several-day period showed good correlation with the northwest-southeast component of wind, which dominated from early summer to fall. This correlation indicates that a temperature decrease is usually induced in the seawater about 2 days after the southeast wind. Furthermore, semidiurnal temperature fluctuation also becomes amplified in the bay about 2 days after the northwest wind. We employed ROMS to clarify these mechanisms, using observed atmospheric conditions and open boundary conditions. After reproducing the temperature variation from spring to fall, we found that over a several-day period, wind could induce water exchange and variation in the temperature difference between water inside and outside of Matsushima Bay.

The temperature difference between water inside and outside of Matsushima Bay was expected to reach a maximum in midsummer; however, it was reduced in July. This was thought to be related to seawater exchange. Combining SST data obtained by the monitoring system, and wind data from AMEDAS, we found that there was a strong correlation between the SST in Matsushima Bay and the southeast-northwest component of the wind. When the wind blew from the southeast, the temperature difference was large. The model indicates that the southeast wind transports warm surface water into the bay, and the northwest wind contributes to the formation of stratification in Matsushima Bay. It was clarified that the wind affected the change in temperature difference during the warming season. Furthermore, the model results revealed that the SST difference between water inside and outside of the bay was frequently induced by wind fluctuation. The appearance of two peaks during the warming season itself is thought to be a type of aliasing feature. Thus, the that there were two peaks is not necessarily important, but research conducted to investigate their characteristics has revealed that wind contributed to seawater exchange in Matsushima Bay. This study showed that small bays such as Matsushima Bay can undergo large changes in sea conditions in a relatively short time. The continuous monitoring system used in this study is very effective tool for accurately gathering data on physical phenomena, such as seawater exchange.

Furthermore, the model results suggest the generation and propagation of internal waves during the period of temperature stratification in Matsushima Bay. From the surface temperature data obtained in the bay, we found that semidiurnal fluctuations were intermittently amplified about 2 days after the southeastward wind blew. This supported our idea that wind could induce seawater exchange and subsequent stratification of Matsushima Bay. In addition, it was shown that wind-induced seawater exchange could move 15% of the volume of Matsushima Bay in 3 days, making it a non-negligible mechanism of seawater exchange in the bay. However, there are some unresolved questions, especially regarding quantitative reproducibility of the details of seasonal variation by the model, and further investigation is needed. To increase the accuracy of the simulation, the influence of rivers must be taken into account. More observation data is required to clarify the effect of internal waves on water mixing.

Acknowledgments

Thanks to the Sena and Vans Corporation for providing us with the monitoring data, and thanks to Shigeho Kakehi, at the Sanyo Techno Marine Company, for providing references. Finally, we would like to thank Mr. Mei from Xiamen University and Dr. Zhou from Tokyo University for discussions about the basic knowledge of numerical computation and ROMS.

References

CHAPMAN, D. C. (1985): Numerical treatment of cross-shelf open boundaries in a barotropic coastal ocean model, J. Phys. Oceanogr., **15**, 1060–1075.

FLATHER, R. A. (1976): A tidal model of the northwest European continental shelf. Memoires de la Societe Royale de Sciences de Liege, **6**, 141–164.

GUO, X. and T. YANAGI (1995): Wind-driven current in Tokyo Bay, Japan during winter. La mer, **33**, 51–64.

GUO, X. and T. YANAGI (1996): Seasonal variation of residual current in Tokyo Bay, Japan —diagnostic numerical experiments. J. Oceanogr, **52**, 597–616.

INTERNATIONAL EMEOS CENTER (2001): The enclosed ocean area in Japan (88 ocean area), environment guidebook.

KAKEHI, S., T. KAMIYAMA, H. ABE, R. MATUSYAMA, A. OSHINO, K. OKABE, K. TAKAYANAGI and K. YOKOUCHI (2017): Mechanisms leading to the decline in Pacific oyster seedlings in Matsushima Bay, Japan. The JSFS 85th Anniversary-Commemorative International Symposium "Fisheries Science for Future Generations", Symposium Proceedings, 01001.

KITADE, Y., M. MATSUYAMA, S. IWATA and I. WATABE (1998): SDP and LP Fluctuations Observed along the Coast of Sagami Bay, J. Oceanogr., **54**, 297–312.

KITADE, Y., and M. MATSUYAMA (2000): Coastal-Trapped Waves with Several-Day Period Caused by Wind along the Southeast Coast of Honshu, Japan. Journal of Oceanogr., **56**, 727–744.

NAGASHIMA, H. and M. OKAZAKI (1979): Observations of temperature, salinity, and current velocity at the mouth of Tokyo Bay in winter. Bull. Coast. Oceanogr.,**16** (2), 76–86 (in Japanese).

SHIRAI, H., R. KUNISATO, S. MAGOME, T. HATTORI, T. TAKAGI, K. OKABE, K. TAKAYANAGI and S. KAKEHI (2019): A High-Resolution Unstructured Grid Finite Volume Model for Currents Around Narrow Straits of Matsushima Bay. In: Oceanography Challenges to Future Earth. Ed. T. Komatsu, HJ. Ceccaldi, J. Yoshida, P. Prouzet, Y. Henocque, p. 161–170, Springer Nature, Switzerland.

WADA, K. (1989): The basic research on characteristics of the tidal field in the enclosed bay. Library in Nagoya University, Nagoya, 156 pp. (in Japanese).

WATANABE K, ABE K, SATO K, SUZUKI K (1972): Current structures in Matsushima Bay -mainly about volume transport and current velocity. Bull. Miyagi Pref. Fish Inst. **6**:89–138 (in Japanese).

WEISS, R. F. (1970): The solubility of nitrogen, oxygen and argon in water and seawater. Deep-Sea Research, **17**, 721–735.

Received: 31 March, 2020
Accepted: 9 June, 2020